Int. j. adv. multidisc. res. stud. 2023; 3(2):699-704

Received: 13-02-2023
Accepted: 23-03-2023

International Journal of Advanced Multidisciplinary Research and Studies

ISSN: 2583-049X

Field Oriented Control for Induction Motor Using Texas Instruments F2806x MCU

Vu Van Thao
Hanoi Industrial Textile Garment University, Hanoi 100000, Vietnam

Corresponding Author: **Vu Van Thao**

Abstract
In the Electric drive system using induction motor requiring high control quality, the field-oriented control (FOC) method is often applied. There have been many studies and applications of the vector control method for 3-phase induction motors in practice. One solution for highly customizable open applications is to use powerful industrial microcontrollers, including the Texas Instruments F2806x MCU. In this paper, the authors implement field-oriented control (FOC) method for induction motor (IM) using F2806x MCU. The theoretical results will be verified experimentally.

Keywords: IM, FOC, F2806x MCU

1. Introduction

In essence, the IM is an object with both structural and parametric nonlinear characteristics [1-6]. When applying the FOC method, isolation control of flux generation and torque generation processes has been realized. IM applications in Industrial are found at every stage of the manufacturing process [7-15], confirming IM motor's critical role as a driving force of production machines. With the V/f control method [16-25], the control algorithm becomes simple, but the system's control quality is not high when the system is mutation load. In drive systems that require high quality using IM, the FOC control method is strictly required. Compared with the PM motor, where the flux has been determined due to the structural nature of the motor [26-33], the FOC structure implemented with the IM motor is more complicated. This study focuses on the responsiveness of the F2806x MCU in implementing FOC control for IM.

2. Mathematical Model of the Three-Phase AC Induction Motor

The stator and rotor flux equations are given below [1]:

$$\begin{cases}\psi_s = L_s i_s + L_m i_r \\ \psi_r = L_m i_s + L_r i_r\end{cases} \tag{1}$$

where$L_s = L_m + L_{\sigma s}$ and $L_r = L_m + L_{\sigma r}$, L_s is the stator inductance, L_r is the rotor inductance, L_m is mutual inductance, $L_{\sigma s}$, $L_{\sigma r}$ is the stator-side and rotor-side dissipation inductances, respectively, is stator current and ir is rotor current. The IM motor in this study is a squirrel cage rotor motor, so the rotor voltage equals zero. Hence, the stator and rotor voltage equations are expressed as follows:

$$u_s = R_s i_s + \frac{d\psi_s}{dt} + j\omega_s \psi_s \tag{2}$$

$$0 = R_r i_r + \frac{d\psi_r}{dt} + j\omega_r \psi_r \tag{3}$$

where ω_r is the slip speed, ω_s is the synchronous speed, ω is the rotor speed.
From the voltage equation and the flux equation we have:

$$\begin{cases} u_s = R_s i_s + \frac{d\psi_s}{dt} + j\omega_s \psi_s \\ 0 = R_r i_r + \frac{d\psi_r}{dt} + j\omega_r \psi_r \\ \psi_s = L_s i_s + L_m i_r \\ \psi_r = L_m i_s + L_r i_r \end{cases} \quad (4)$$

Eliminating the rotor current and the stator flux from (4), we obtain the following equations on the dq coordinate system as below:

$$\begin{cases} \frac{di_{sd}}{dt} = -\left(\frac{1}{\sigma T_s} + \frac{1-\sigma}{\sigma T_s}\right) i_{sd} + \omega_s i_{sq} + \frac{1-\sigma}{\sigma T_r} \psi'_{rd} + \frac{1-\sigma}{\sigma} \omega \psi'_{rq} + \frac{1}{\sigma L_s} u_{sd} \\ \frac{di_{sq}}{dt} = -\omega_s i_{sd} - \left(\frac{1}{\sigma T_s} - \frac{1-\sigma}{\sigma T_r}\right) i_{sq} - \frac{1-\sigma}{\sigma} \omega \psi'_{rq} + \frac{1-\sigma}{\sigma T_r} \psi'_{rq} + \frac{1}{\sigma L_s} u_{sq} \\ \frac{d\psi'_{rd}}{dt} = \frac{1}{T_r} i_{sd} - \frac{1}{T_r} \psi'_{rd} + (\omega_s - \omega) \psi'_{rq} \\ \frac{d\psi'_{rd}}{dt} = \frac{1}{T_r} i_{sq} - (\omega_s - \omega) \psi'_{rd} - \frac{1}{T_r} \psi'_{rq} \end{cases} \quad (4)$$

Select the rotating *dq* coordinate system whose *q* axis is perpendicular to the flux generated by the rotor, we have $\psi_{rd} = 0$. Applying this to (5) yields:

$$\frac{di_{sd}}{dt} = -\left(\frac{1}{\sigma T_s} + \frac{1-\sigma}{\sigma T_s}\right) i_{sd} + \omega_s i_{sq} + \frac{1-\sigma}{\sigma T_r} \psi'_{rd} + \frac{1}{\sigma L_s} u_{sd} \quad (5)$$

$$\frac{di_{sq}}{dt} = -\omega_s i_{sd} - \left(\frac{1}{\sigma T_s} - \frac{1-\sigma}{\sigma T_r}\right) i_{sq} - \frac{1-\sigma}{\sigma} \omega \psi'_{rd} + \frac{1}{\sigma L_s} u_{sq} \quad (6)$$

$$\frac{d\psi'_{rd}}{dt} = \frac{1}{T_r} i_{sd} - \frac{1}{T_r} \psi'_{rd} \quad (7)$$

$$0 = \frac{1}{T_r} i_{sq} - (\omega_s - \omega) \psi'_{rd} \quad (8)$$

Accordingly, we can determine the equation for moment of force and the equations for the calculation and for the control of the rotor flux:

$$m_M = \frac{3}{2} z_p (1-\sigma) L_s \psi'_{rd} i_{sq} \quad (9)$$

and

$$0 = i_{md} + T_r \frac{di_{md}}{dt} - i_{sd} \quad (10)$$

$$0 = \omega_r T_r i_{md} - i_{sq} \quad (11)$$

$$i_{md} = \frac{\psi_{rd}}{L_m} \quad (12)$$

Thus, the control quantity for flux is i_{sd}, and the control quantity for the moment of force is i_{sq}.

3. Space vector modulation and formulas to convert the coordinate system

The space vector modulation (SVM) method is based on the stator voltage equation (13) with the condition (14). By presenting the stator voltage equation as a vector, it is easy to control the IM motor based on imposing a three-phase voltage on the stator.

$$u_s = \frac{2}{3}\left(u_a(t) + u_b(t) + u_c(t)\right) \quad (13)$$

$$u_a(t) + u_b(t) + u_c(t) = 0 \quad (14)$$

Unlike u_a, u_b, u_c, the vector u_s is a vector with constant modules with the angular frequency determined on the Oxy plane with the Ox axis coinciding with the phase *a*. This vector can be represented as two orthogonal vectors *ux* and *uy* by projecting on an arbitrary *Odq* coordinate system. Accordingly, u_s can be expressed as below:

$$\overrightarrow{u_s} = \overrightarrow{u_x} + \overrightarrow{u_y} \quad (15)$$

In the FOC control method, it is common to choose two common coordinate systems. The Oαβ-coordinate system has the α-axis coinciding with the windings of phase *a*, known as a fixed coordinate system with the stator. The *Odq* coordinate system has the *d* axis coinciding with the rotor flux angle, known as the rotor flux coordinate system. Therefore, to carry out the IM motor control as described in equations (10), (13), it is necessary to convert the measured current and voltage to the *dq* coordinate system and convert the control signal from the *dq* coordinate system to the αβ coordinate system.
The formula for converting the current from *αβ* coordinate system to *abc* coordinate system is given as

$$\begin{bmatrix} i_\alpha \\ i_\beta \end{bmatrix} = \frac{2}{3}\begin{bmatrix} 1 & -\frac{1}{2} & -\frac{1}{2} \\ 0 & \frac{\sqrt{3}}{2} & -\frac{\sqrt{3}}{2} \end{bmatrix} \times \begin{bmatrix} i_a \\ i_b \\ i_c \end{bmatrix} \tag{16}$$

The formula for converting the current from *αβ* coordinate system to *dq* coordinate system is

$$\begin{bmatrix} i_d \\ i_q \end{bmatrix} = \begin{bmatrix} cos(\varphi) & sin(\varphi) \\ -sin(\varphi) & cos(\varphi) \end{bmatrix} \times \begin{bmatrix} i_\alpha \\ i_\beta \end{bmatrix} \tag{17}$$

The formula for converting the voltage from *dq* coordinate system to *αβ* coordinate system is

$$\begin{bmatrix} u_d \\ u_q \end{bmatrix} = \begin{bmatrix} cos(\phi) & -sin(\phi) \\ sin(\phi) & cos(\phi) \end{bmatrix} \times \begin{bmatrix} u_\alpha \\ u_\beta \end{bmatrix} \tag{18}$$

The formula for converting the voltage from *αβ* coordinate system to *abc* coordinate system is

$$\begin{bmatrix} u_a \\ u_b \\ u_c \end{bmatrix} = \begin{bmatrix} 1 & 0 \\ -\frac{1}{2} & \frac{\sqrt{3}}{2} \\ -\frac{1}{2} & -\frac{\sqrt{3}}{2} \end{bmatrix} \times \begin{bmatrix} u_\alpha \\ u_\beta \end{bmatrix} \tag{19}$$

The F2806x MCU is designed for motor control applications. Therefore, they are optimized for these applications with the library blocks available for the above transformation.

4. Algorithm for flux model

The method of determining the rotor flux uses an equation

$$\psi_{rd} = L_m \int \left(\frac{1}{T_r} i_{sd} - \frac{1}{T_r}\psi_{rd}\right) dt \tag{20}$$

For ease of application to microcontrollers, the above equation is discretized as follows:

$$\psi_{rd}(k) = L_m\left(\frac{T_s}{T_r} i_{sd}(k-1) - \left(1 - \frac{T_s}{T_r}\right)\psi_{rd}(k-1)\right) \tag{21}$$

The condition for the correct expression (22) is that the *dq* coordinate system must be in sync with the rotor flux's rotation angle, and the *d* axis must coincide with the direction of the flux vector. We can determine the value of the synchronous angular velocity as follows:

$$\omega_s = \frac{1}{T_r}\frac{i_{sq}}{\psi_{rd}} + z_p\omega \tag{22}$$

Discretizing the above equation yields:

$$\omega_s(k+1) = \frac{1}{T_r}\frac{i_{sq}(k-1)}{\psi_{rd}(k-1)} + z_p\omega(k-1) \tag{23}$$

In practice, acquiring parameters such as ia, ib always uses low pass filters, so the measured current signals will be phase lag compared to the actual current. The obtained flux angle of the model will be delayed by a certain value compared to the actual flux angle. To have the correct angle, it is necessary to have an angle correction stage before putting it into the voltage coordinate conversion.

5. Experimental results

An experimental model built upon the descriptions given using F2806x MCU is used to execute the control algorithm. The entire controller structure has been designed on Matlab / Simulink software and compiled to be included in the microcontroller. The results are given in Fig 1 to Fig 3.

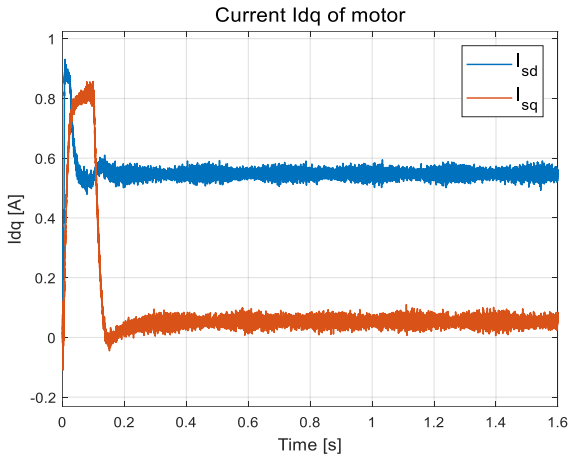

Fig 1: Experimental results of current Idq

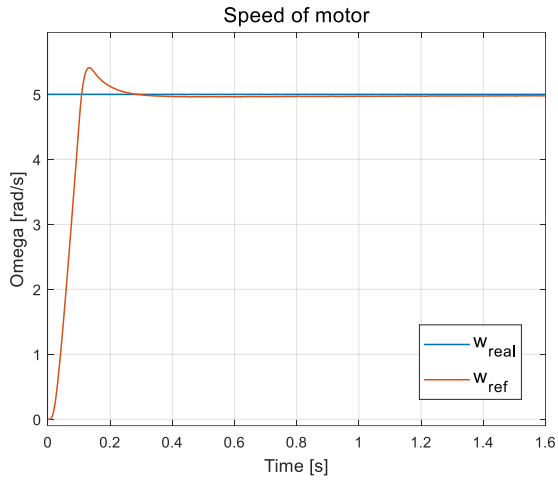

Fig 2: Experimental results of the speed

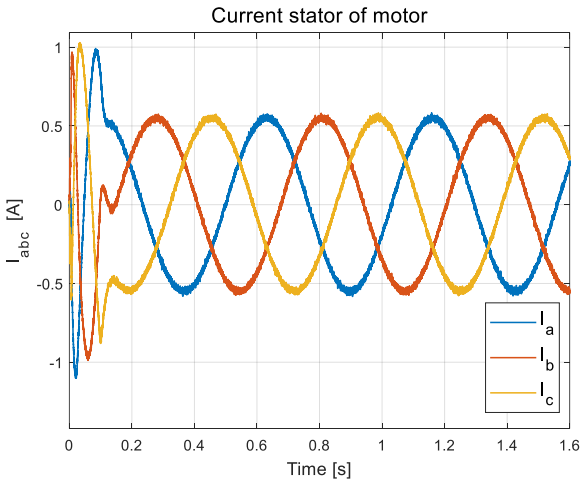

Fig 3: Experimental results of the current

6. Conclusion

The obtained experimental results confirm that F2806x MCU can implement the FOC control technique for IM motors. In particular, the meaning of the IM control systems developed on the F2806x MCU is low cost. The author proposes a solution to build a standardized hardware system that can interfere with the microprocessor's control structure. The advantage of this solution is that it is inexpensive and allows us to install different algorithms. Besides, the researcher can adequately intervene in the system.

7. Acknowledgements

The author acknowledges the Hanoi Industrial Textile Garment University for supporting this works.

8. References

1. Quang NP, Dittrich JA. Vector Control of Three-Phase AC Machines: System Development in the Practice, 2016.
2. Gao J, Zhang L, Wang X. AC machine systems. Mathematical Model and Parameters, Analysis, and System Performance, 2009.
3. Boldea I, Nasar SA. Vector control of AC drives. CRC press, 1992.
4. Abu-Rub H, Iqbal A, Guzinski J. High performance control of AC drives with Matlab/Simulink. John Wiley & Sons, 2021.
5. Bakshi UA, Bakshi MV. Electrical Machines-I. Technical Publications, 2020.
6. Trzynadlowski AM. Control of induction motors. Elsevier, 2000.
7. Liang X, Ilochonwu O. Induction motor starting in practical industrial applications. IEEE Transactions on Industry Applications. 2010; 47(1):271-280.
8. Jacobina CB, De Rossiter Correa MB, Da Silva EC, Lima AMN. Induction motor drive system for low-power applications. IEEE Transactions on Industry Applications. 1999; 35(1):52-61.
9. Lopez-Perez D, Antonino-Daviu J. Application of infrared thermography to failure detection in industrial induction motors: case stories. IEEE Transactions on Industry Applications. 2017; 53(3):1901-1908.
10. Diab AAZ, Al-Sayed AHM, Abbas Mohammed HH, Mohammed YS, Diab AAZ, Al-Sayed AHM, *et al*. Literature review of induction motor drives. Development of Adaptive Speed Observers for Induction Machine System Stabilization, 2020, 7-18.
11. Lee YO, Jo J, Hwang J. Application of deep neural network and generative adversarial network to industrial maintenance: A case study of induction motor fault detection. In 2017 IEEE international conference on big data (big data), December 2017, 3248-3253. IEEE.
12. Abrahamsen F, Blaabjerg F, Pedersen JK, Grabowski PZ, Thogersen P. On the energy optimized control of standard and high-efficiency induction motors in CT and HVAC applications. IEEE Transactions on Industry Applications. 1998; 34(4):822-831.
13. Blaabjerg F, Lungeanu F, Skaug K, Tonnes M. Evaluation of low-cost topologies for two phase induction motor drives, in industrial applications. In Conference Record of the 2002 IEEE Industry Applications Conference. 37th IAS Annual Meeting (Cat. No. 02CH37344). October 2002; 4:2358-2365. IEEE.
14. Cirrincione M, Pucci M, Cirrincione G, Capolino GA. A new experimental application of least-squares techniques for the estimation of the induction motor parameters. IEEE Transactions on Industry Applications. 2003; 39(5):1247-1256.
15. Zhang P, Du Y, Habetler TG, Lu B. A survey of condition monitoring and protection methods for medium-voltage induction motors. IEEE Transactions on Industry Applications. 2010; 47(1):34-46.
16. Munoz-Garcia A, Lipo TA, Novotny DW. A new induction motor V/f control method capable of high-performance regulation at low speeds. IEEE transactions on Industry Applications. 1998; 34(4):813-821.
17. Koga K, Ueda R, Sonoda T. Constitution of V/f control for reducing the steady-state speed error to zero in induction motor drive system. IEEE transactions on industry applications. 1992; 28(2):463-471.
18. Zhang Z, Liu Y, Bazzi AM. An improved high-performance open-loop V/f control method for induction machines. In 2017 IEEE Applied Power Electronics Conference and Exposition (APEC), March 2017, 615-619). IEEE.
19. Pimkumwong N, Wang MS. Full-order observer for direct torque control of induction motor based on constant V/F control technique. ISA transactions. 2018; 73:189-200.
20. Habbi HMD, Ajeel HJ, Ali II. Speed control of induction motor using PI and V/F scalar vector controllers. International Journal of Computer Applications. 2016; 151(7):36-43.
21. Peña JM, Díaz EV. Implementation of V/f scalar control for speed regulation of a three-phase induction motor. In 2016 IEEE ANDESCON , October 2016, 1-4. IEEE.
22. Suzuki K, Saito S, Kudor T, Tanaka A, Andoh Y. Stability improvement of V/F controlled large capacity voltage-source inverter fed induction motor. In Conference Record of the 2006 IEEE Industry Applications Conference Forty-First IAS Annual Meeting. October 2006; 1:90-95. IEEE.
23. Reddy MHV, Jegathesan V. Open loop V/f control of induction motor based on hybrid PWM with reduced torque ripple. In 2011 International Conference on Emerging Trends in Electrical and Computer Technology, March 2011, 331-336. IEEE.
24. Chitra A, Vanishree J, Sreejith S, Jose S, Pulickan AJ. Performance comparison of multilevel inverter topologies for closed loop v/f controlled induction motor drive. Energy Procedia. 2017; 117:958-965.
25. Mahato B, Jana KC, Thakura PR. Constant V/f control and frequency control of isolated winding induction motor using nine-level three-phase inverter. Iranian Journal of Science and Technology, Transactions of Electrical Engineering. 2019; 43:123-135.
26. Morimoto S, Takeda Y, Hirasa T. Current phase control methods for permanent magnet synchronous motors. IEEE Transactions on Power Electronics. 1990; 5(2):133-139.
27. Ullah K, Guzinski J, Mirza AF. Critical review on robust speed control techniques for permanent magnet synchronous motor (PMSM) speed regulation. Energies. 2022; 15(3):1235.
28. Cheng B, Tesch TR. Torque feedforward control technique for permanent-magnet synchronous motors. IEEE Transactions on Industrial Electronics. 2010; 57(3):969-974.
29. Jahns TM. Motion control with permanent-magnet AC machines. Proceedings of the IEEE. 1994; 82(8):1241-1252.
30. Li S, Xia C, Zhou X. Disturbance rejection control method for permanent magnet synchronous motor speed-regulation system. Mechatronics. 2012; 22(6):706-714.
31. Gieras JF. Permanent magnet motor technology: design and applications. CRC press, 2002.

32. Vaez-Zadeh S. Control of permanent magnet synchronous motors. Oxford University Press, 2018.
33. Furlani EP. Permanent magnet and electromechanical devices: materials, analysis, and applications. Academic press, 2001.